A MATHEMATICAL MODEL OF RELATION AND ORIGIN OF VARIATION BETWEEN CRI AND CSR INDEXES

Danil Alekseev[a], Andrey Smirnov[b], Konstantin Chalyy[b]

[a)]National University of Science and Technology (MISiS), Novotroitsk, Orenburg region, st. Frunze 8, 462359, Russia,
[b)]Nosov Magnitogorsk State Technical University, Chelyabinsk region, Lenin Avenue 38, Magnitogorsk, 455000
alekseev41047@mail.ru

The aim of this work is both the mathematical relation and the value variation analysis between CRI and CSR indexes. For this aim the physical mathematical model is proposed on the basis of the ISO-test. The physical basis of the model is a material balance of a one piece of coke from the ISO sample. Results of calculating by the model are curves of $CSR = f(CRI)$ which reproduces the regressions in analogy with $CSR = a + b * CRI$ for most coke-producing countries. The model showed that a larger part of CSR=f(CRI) curve is linear and that a universal regression in analogy with $CSR = a + b * CRI$ does not exist. As follows from the model, every piece of coke from the ISO sample has its own CSR=f(CRI) curve with a CRI and CSR point. Between pieces of coke, variations of CRI and CSR values can be explained by the open pore amount, the coke pores' surface area, the statistical distribution of molecular oriented domains on the basis of Lc and the coke piece mass. In our results, pores with a geometrical orientation from the outside to the center of a coke piece and having a minimum length significantly influence on the coke quality according to CRI and CSR indexes.

Key words: coke, NSC test, coke strength after reaction, coke reactivity, mathematical physical model; open and closed pores, molecular oriented domains

Received 18. 07. 2021, Accepted 23. 08. 2021

1. Introduction

Nowadays the majority of metallurgy companies in the world are using the two-stage technology of steel making which consists of the blast-furnace cast-iron smelting and various methods of its conversion to steel. Coke is a critical component of the blast-furnace production. The coke quality by the mechanical strength influences the capacity of the blast furnace [1]. There are many standards for assessing the coke mechanical strength quality. Currently, the NSC-test in the ISO form (ISO-test) is popular with researchers. The outcomes of the ISO-test are the CRI and CSR indexes. There are many models for predicting CRI and CSR indexes from different variables and there are many linear regressions in the form of $CSR = a + b * CRI$ [2-4]. Also, the modernized CRI and CSR indexes are in [5].

The science of coke has accumulated many experimental facts about the coke quality formation. There are many good models describing the coke quality formation in relation to coal parameters. However, in our opinion, at present, the fundamental theory of the coke quality formation has not been created. Let's give an example. Newton's second law is a fundamental formula. There is no need to check the law, it will be valid for any macro body at speeds much lower than the speed of light in a vacuum. On the other hand, if any mathematical model for predicting coke quality indicators is tested on coals that were not taken into account while creating this model, then it is likely that the calculation results will diverge from practical data. In our opinion, it is impossible to improve coke production and processing technologies without a fundamental theory. In addition, an important issue in coke chemistry is the question of what is considered an indicator of coke quality. We will explain what has been said. All methods or standards for assessing the coke mechanical strength quality have a general physical basis which is a revolving drum with pieces of coke. From the general physical basis, a universal formula must exist for transforming one mechanical strength index to another. A similar remark applies to the NSC test. For example, we will propose new indexes if we change the coke size from 19.0-22.4 mm to 30-40 mm or the drum dimension within the ISO-test. Thus, there must be a general formula for the transition from one coke quality indicator to another. There is still the question, which of the indicators is considered optimal or rational for determining coke quality indicators.

In this work, we pursue to generalize the existing results of the coke physical structure studies based on our model. We provide in the article a detailed construction of our model from hypotheses to the configuration of dependences CSR = f (CRI) (Appendix A), discussion of hypotheses (Appendix B) and simulation results (Section 3). Such a presentation, in our opinion, allows us to formulate new questions on the coke quality formation, which are still poorly studied.

The model is based on hypotheses. On the one hand, our hypotheses are contentious, some of which currently require targeted testing, for example, the distribution of molecular-oriented domains (MOD) or the apparent density distribution inside a piece of coke. On the other hand, the model makes it possible to explain a number of important facts, specifically, the linearity between CRI and CSR, variation in CRI and CSR values, and the absence of a universal regression like $CSR = a + b * CRI$. We

consider our work as an attempt to make a contribution to the footing of the coke quality theory.

2. A mathematical model of relation between CRI and CSR

2.1. Physical basis of the model

The ISO-test on CRI and CSR can be provisionally divided into three stages. At the first stage, pieces of coke with a total mass of 200 grams and a diameter of 19.0–22.4 mm are being prepared. Within the model we assume that any piece of coke for the ISO-test is a ball with a r_0 radius and its apparent density of $\rho(r)$ is evenly distributed along the radius before the reaction with CO_2 (Fig. 1).

The apparent density of the coke from coals of Russia and countries of the former Soviet Union is in the range of 0.8-0.9 g/m^3 [6]. Within the model for calculations, we take the mean value of ρ_{ad}=0.85 g/cm^3. The $\rho_{ad} = 0.85\ g/cm^3$ value in our calculations was taken for demonstration purposes. The curve trajectory while changing ρ_{ad} will remain the same, but the values of A and r'_0 will change (section 2.2., Appendixes A and B). To determine A and r'_0, it is necessary to know the parameters of r_0^x, r_x and m_2, which are problematic to observe in practice (section 3, Appendixes A and B). At the same time, the variation of coke quality indicators based on the apparent density alone cannot be explained, and it is clear from formulas (I - V) (section 3).

At the second stage, to determine the CRI index, coke pieces react with CO_2 at the temperature of 1100 ^{0}C. We suppose that the geometrical shape of a coke piece after its reaction with CO_2 is unaltered, that is coke carbon weight loss is much greater on the inner surface area of coke pores than on the outside surface of a coke piece. Based on this assumption, after the reaction, the apparent density distribution in a piece of reacted coke has a linear type depending on radius (Fig. 2).

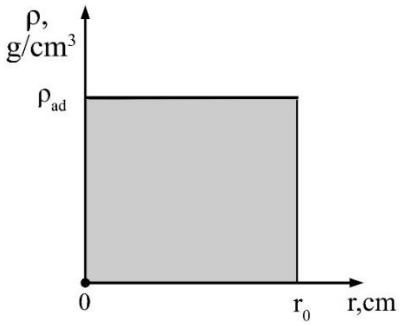

Fig. 1. Distribution of apparent density $\rho(r)$ depending on radius in a spherical coke piece before the reaction with CO_2

At the third stage, to determine the CSR index, the entire mass of reacted coke is transferred to a cylindrical drum with a length of 700 mm and an inner diameter of 130 mm. After 600 revolutions for 30 minutes, all coke pieces are sifted through a 10 mm screen.

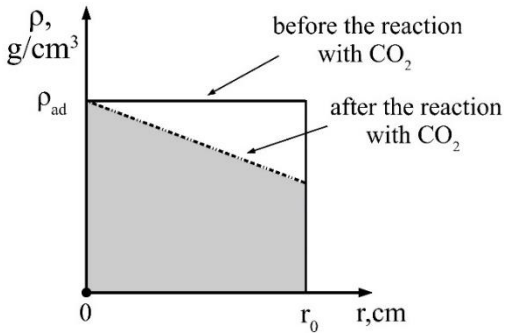

Fig. 2. Distribution of apparent density $\rho(r)$ depending on radius before and after the reaction with CO_2 (Fig. 2 is an individual case, Fig. A.5 in Appendix A is a general case)

The coke pieces with a diameter larger than 10 mm are found quite suitable. The third stage results according to the model are shown in the Fig. 3.

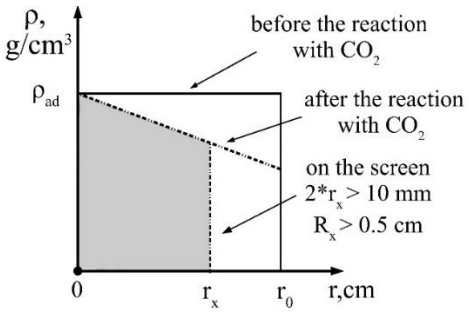

Fig. 3. Apparent density distribution $\rho(r)$ depending on radius after the drum test

CRI and CSR indexes are relative values calculated on the basis of a 200 g coke sample. We assume that CRI and CSR values can be used both to a 200 g coke sample and to the entire mass of coke within the sample. Therefore, we constructed the model according to the following hypotheses:

1. All the coke pieces within a 200 g sample are spherical;
2. The distribution of apparent density $\rho(r)$ depending on radius is linear for all coke pieces after the reaction with CO_2.
3. Coke carbon weight loss is much greater on the inner surface of coke pores in comparison with that on the outside surface of a coke piece. The shape and radius of a coke piece are constant after the reaction with CO_2.
4. CRI and CSR values are equal for all coke pieces within a 200 g sample for the ISO-test. In a different way, the CRI and CSR indexes from the ISO-test can be used to the entire coke piece.
5. After the reaction and the drum test apparent density distributions $\rho(r)$ depending on radius are equal for all coke pieces within a 200 g sample for the ISO-test.

2.2. Mathematical basis of model

The mathematical model of the relation between CRI and CSR (Appendix A and B) obtained on the physical basis (section 2.1) consists of:

$$m_1 = 4\pi\left(k\frac{{r_0}^4}{4} + (\rho_{ad} + k{r'}_0)\frac{{r_0}^3}{3}\right) \text{ (I)}$$

$$r_x = r_0^x\frac{1}{1+(A*k)^2} + {r'}_0\left(\frac{1}{1+(A*k)^2} - 1\right) \text{ (II)}$$

$$m_2 = 4\pi\left(k\frac{{r_x}^4}{4} + (\rho_{ad} + k{r'}_0)\frac{{r_x}^3}{3}\right) \text{ (III)}$$

$$CRI = 100\frac{m_0 - m_1}{m_0} \text{ (IV)}$$

$$CSR = 100\frac{m_2}{m_1} \text{ (V)}$$

In the set of (I – V), equations (I – III) are mathematical independent, and (IV – V) are dependence from (I – III). In (I – V), unknown variables are ${r'}_0$, A and k. Variables of r_0, ρ_{ad}, m_0 and m_1 can be observed for all coke pieces within a 200 g sample going to the ISO-test [8]. Variables of r_0^x, r_x and m_2 are unobserved in the ISO-test because of the problem with the coke piece marking before and after the drum test (Appendix A and B).

The algorithm for modeling the relation between CRI and CSR within the set of (I – V) is below (all values are given as an example in the algorithm):

1. Enter $\rho_{ad} = 0.85$ (g/cm^3); $r_0 = 1.05$ (cm); $r_0^x = 1.03$ (cm) (values can be varied);
2. Enter ${r'}_0$. For example, ${r'}_0 = 0$ (cm);
3. Calculate $m_0 = \frac{4}{3}\pi r^3\rho_{ad}$;
4. $i \in [0; 100]$ $step$ 1;
5. $CRI_i = i$, $CRI_i \in [0; 100]$;
6. Calculate $(m_1)_i = m_0 - \frac{m_0 * CRI_i}{100}$;
7. Calculate
   $k_i = \left(\frac{(m_1)_i}{4\pi} - \frac{\rho_{ad}*{r_0}^3}{3}\right) * \left(\frac{{r_0}^4}{4} + +{r'}_0\frac{{r_0}^3}{3}\right)^{-1}$
   (see formula (I));
8. $A_i \in [2; 4]$ (A_i can take any value provided $A_i > 0$);
9. $j \in [0; 100]$ $step$ 1;
10. Calculate
    $$(r_x)_{i,j} = r_0^x\frac{1}{1 + \left(A_j k_i\right)^2} + +{r'}_0\left(\frac{1}{1 + \left(A_j k_i\right)^2} - 1\right)$$
    First runs i, then j changes;
11. Calculate
    $$(m_2)_{i,j} = 4\pi\left(\frac{k_i}{4}{(r_x)_{i,j}}^4 + (\rho_{ad} + +k{r'}_0)\frac{{(r_x)_{i,j}}^3}{3}\right).$$
    First runs i, then j changes;
12. Calculate $(CSR)_{i,j} = 100\frac{(m_2)_{i,j}}{(m_1)_i}$.
    First runs i, then changes j;
13. Print curves of $CSR = f(CRI)$ (one curve at $j = const$). Select j (the choice of A_j value) so that the curve goes through an experimental point of (CRI; CSR);
14. If printed curves of $CSR = f(CRI)$ does not go through an experimental point of (CRI; CSR) then ${r'}_0$ must be changed and the algorithm goes to the beginning.
15. The calculation ends.

3. The results and discussion

3.1. General form curve of $CSR = f(CRI)$

The general form curve of $CSR = f(CRI)$ calculated by the model is shown in Fig. 4. The main parts of the curve are given in Fig. 5. The course of the ISO-test imposes restrictions on the curve (Fig. 5):

1. The curve is physical at $r_x > 0.5$. A coke piece goes through the screen at $r_x < 0.5$ and has $CSR = 0$;
2. The curve of $CSR = f(CRI)$ should not have increasing portions. Increasing portions of the curve demonstrate that the rate of a coke piece destruction decelerates with increasing CRI which is not true.

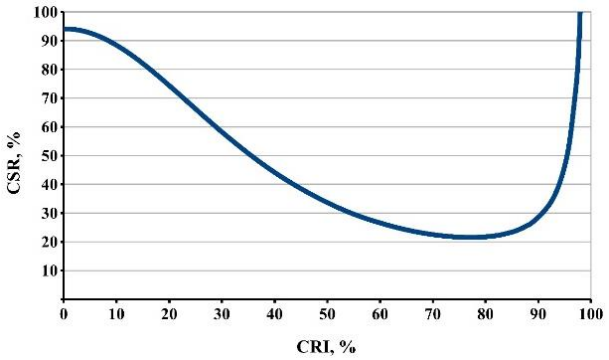

Fig. 4. General form curve of $CSR = f(CRI)$ at modelling (for this curve: $\rho_{ad} = 0.85$, $r_0 = 1.05$, ${r'}_0 = 0$, $r_0^x = 1.03$, $A = 1{,}4$, $r_x > 0{,}5$ at $CRI \leq 68\%$)

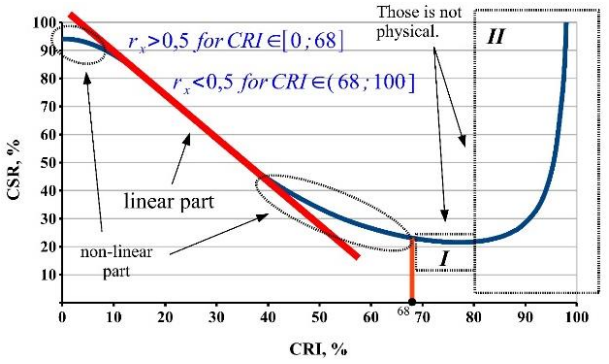

Fig. 5. The main parts of the curve (for this curve: $\rho_{ad} = 0.85$, $r_0 = 1.05$, ${r'}_0 = 0$, $r_0^x = 1.03$, $A == 1.4$, $r_x > 0.5$ at $CRI \leq 68\%$)

In appendix A, formula (A.40) demonstrates that the curve has both linear and non-linear parts. Linear parts are located in the center of the curve, and non-linear ones are on edges (Fig. 5). Thus, according to the model the larger part of the curve $CSR = f(CRI)$ is linear.

3.2. Variation of regressions in terms of $CSR = a + b * CRI$

Figs. 6–12 demonstrate regressions provided by scientists around the world (regressions and countries are

represented in the Table) as well as the results of modelling. For comparison, Figures 6–12 coincide with the data from [5,9]. In [5], cokes are produced from coal blends at Chinese plants. In [9], cokes are manufactured from Polish coals in laboratory conditions from binary and ternary coal blends. Fig. 6 demonstrates the possibilities of modelling curves by the model.

Usually linear regressions are based on some narrow range of CRI and CSR data [2, 3]. On what ranges the regressions shown in the table were built is not known now. Typically, this range is from 20 to 60%.

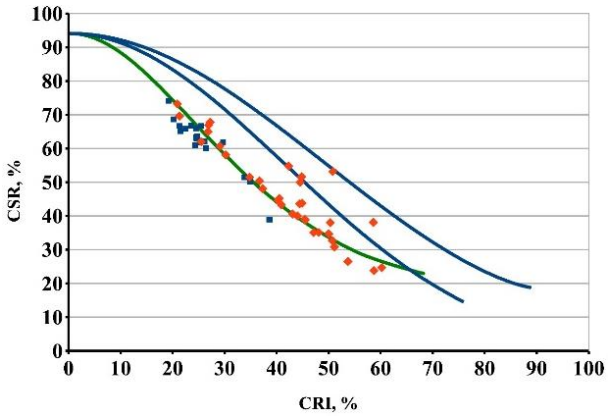

Fig. 6. Possibilities of modelling curves by the model (blue points are from Chinese research [5]; red points are from Polish research [9]

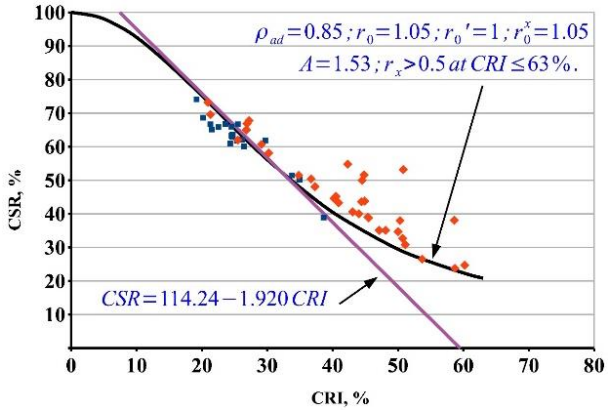

Fig. 7. Regression from Russian research ($CSR = 114.24 - 1.920CRI$) and the results of modelling (blue points are from Chinese research [5]; red points are from Polish research [9]; points for comparison)

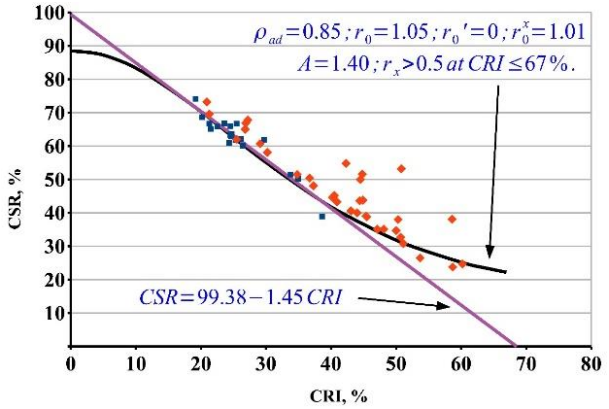

Fig. 8. Regression and blue points from Chinese research ($CSR = 99.38 - 1.45CRI$ [5] and the results of modelling (red points are from Polish research [9]; points for comparison)

Table of regressions by type $CSR = linear(CRI)$ with a great variation of coefficients [10]

Country	Regressions	$CSR = a + b * CRI$	
		$CSR(0) = a$	$0 = a + b * CRI$ $CRI = -a/b$
Russia	$CSR = 114.24 - 1.920CRI$	114.24	59.5
China	$CSR = 99.38 - 1.45CRI$	99.38	68.5
Ukraine	$CSR = 86.2 - 1.175CRI$	86.2	73.4
Germany	$CSR = 87.74 - 0.9771CRI$	87.74	89.8
Canada	$CSR = 86.879 - 1.046CRI$	86.879	83.1
Japan	$CSR = 80.89 - 0.8523CRI$	80.89	94.9

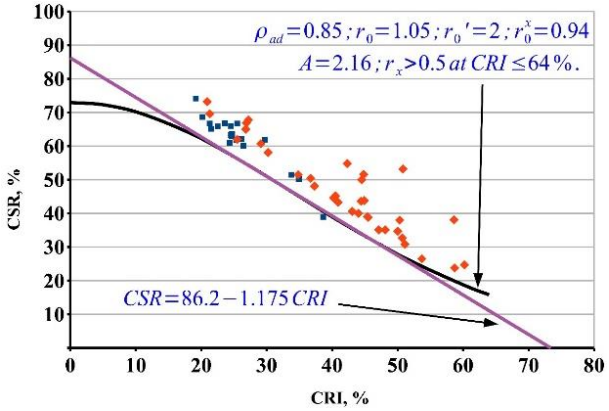

Fig. 9. Regression from the Ukrainian research ($CSR = 86.2 - 1.175CRI$) and the results of modelling (blue points are from Chinese research [5]; red points are from Polish research [9]; points for comparison)

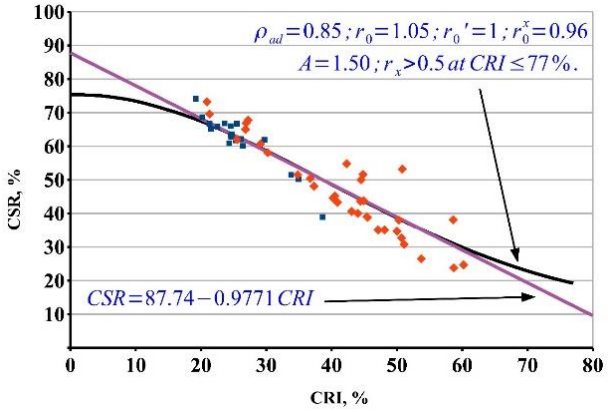

Fig. 10. Regression from German research ($CSR = 87.74 - 0.9771CRI$) and the results of modelling (blue points are from Chinese research [5]; red points are from Polish research [9]; points for comparison)

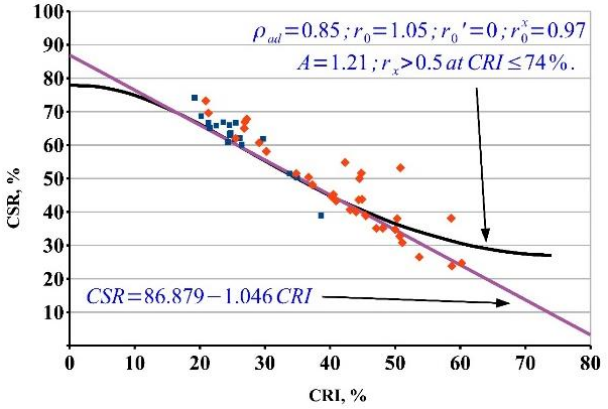

Fig. 11. Regression from Canadian research ($CSR = 86.879 - 1.046CRI$) and the results of modelling (blue points are from Chinese research [5]; red points are from Polish research [9]; points for comparison)

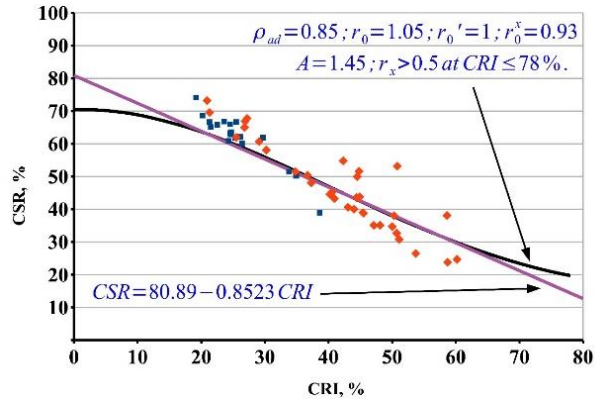

Fig. 12. Regression from Japanese research ($CSR = 80.89 - 0.8523CRI$) and the results of modelling (blue points are from Chinese research [5]; red points are from Polish research [9]; points for comparison)

According to the statistics rules regression cannot be used beyond the limits of the given range. For instance, for Russian regression, let's consider the point $CSR(0) = 114.24\%$ (table). It turns out that if you do not carry out the reaction ($CRI = 0$) and rotate the coke sample, then $CSR = 114.24\%$. This is physically meaningless because CSR is 100% max. That is, the regression lines at the ends are meaningless. They are valid approximately in the range from 20 to 60%. When we model the $CSR = f(CRI)$ curves, they have linear and non-linear parts. The linear part coincides with the regression (there is no need for a correlation coefficient), and the non-linear part behaves correctly. Thus, for small values of CRI, close to "0", the mechanical strength of CSR will vary slightly, which is correctly reflected on the curves. Since formulas (I) - (V) generate all the regression curves without being linear, it can be concluded that there is no universal linear regression.

3.3. Variations of CRI and CSR values

3.3.1 Influence and physical interpretation of the coefficient A

The model has coefficients r'_0 and A without any physical manifestation (see formulas I–V, Appendixes A and B). We give our interpretations of these coefficients. Within formulas (I–V), only formula (II) for calculating r_x contains the coefficient A. The coefficient A has no relation to m_2 and CSR, but is linked with m_1 and CRI. The model yields that the larger the value of A the shorter will be the curve of $CSR = f(CRI)$ and less the value of CSR at $CRI = const$ (Fig. 13).

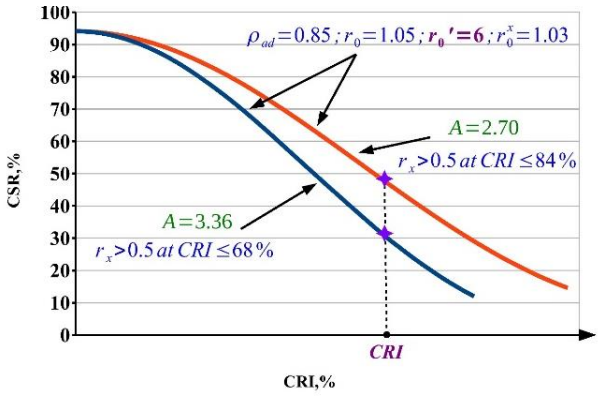

Fig. 13. Influence of coefficient A on the curve in the model

Coefficient A in the model has the dimension that is cm^4/g (formulas (A.4) and (A.35) in **Appendix A**). The dimension of cm^4/g is:

$$\left[\frac{\text{cm}^4}{g}\right] = \left[\frac{g}{cm^3}\right]^{-1} * [cm]$$

From this, we can assume that:

$$A \sim \frac{1}{\rho} * l$$

We suggest that the density of ρ can be considered as the true coke density, and l is a linear dimension corresponding to a measure of length, for example, 1 mm or 1 nm. Density refers to the coke material. The proportionality factor A is included in the equation (II), that is, it is

related to r_x, m_2 and the coke strength CSR. Molecular-oriented domains (MOD) are the coke body material (related to density from the A coefficient), which is precisely what provides the coke strength properties (CSR). Thus, A can be physically linked to the MOD. If the length of l is fixed and the density of ρ increases, the value of A decreases. Vice versa, if ρ decreases at $l = const$, A increases. For this reason, CSR coke strength is larger at the larger of ρ and the lower of A (Fig. 13).

The true coke density may depend on the amount and coal ash composition, but during cokemaking from one coal batch with fixed ash, the true coke density might variate in different parts of the coking chamber [11]. Continue the reasoning, 10 molecular oriented domains (MOD) with a 1 nm length or 1 MOD with a 10 nm length can be within the length of 10 nm. True coke density is larger with 1 MOD of a 10 nm length, because 10 MOD with a 1 nm length have interfacial joints with less true density. Therefore, the value of A at 1 MOD with a length of 10 nm is less then at 10 MOD with a length of 1 nm, and CSR is larger (Fig. 13). We guess that values of A are connected with a MOD statistical distribution of L_c in coke. The earlier researches related values of L_c with CSR [11, 12]. The results of this research are shown in Fig. 14. A group of points in Fig. 14 deviates from the general trend of CSR (CSR points are 59.2, 56.3, 60.0, 57.4, 59.6 %). This group of points has an approximately similar surface area value (hence, CRI is an approximately const) and different L_c values. The amount of MOD in coke is enormous. In the analytical procedure, a value of L_c is a mean value [12].

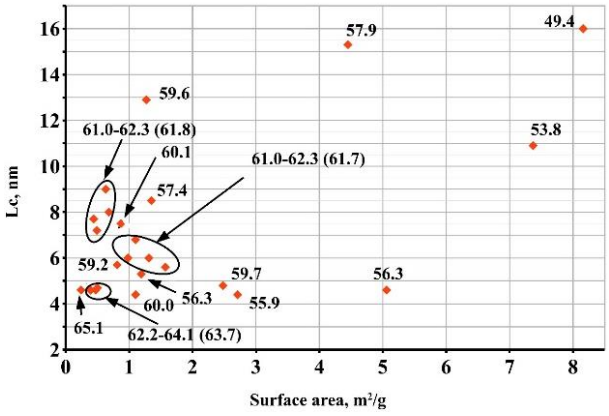

Fig. 14. A relation between the surface area, the MOD crystallite height of Lc and CSR (values alongside points). Data from [11]

Diagrammatically, the Figure 15 shows an assumed distribution of L_c on the basis of Gauss distribution. If the weight loss of I and II patterns is constant, the amount of particles with less values of L_c decreases (Fig. 16).

Distributions in Fig. 16 are approximate, as not only small MOD react with CO_2 but large MOD as well. In reality the distribution may take the form as given in Fig. 15 or as in Fig. 15 but with a kurtosis.

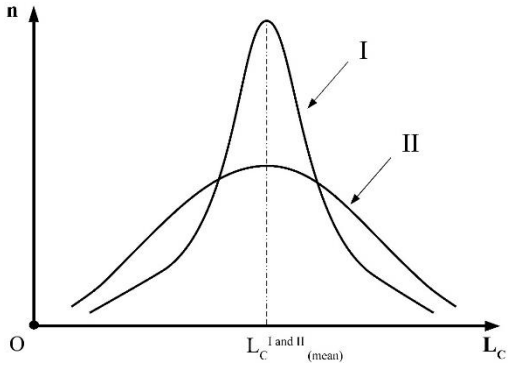

Fig. 15. An assumed distribution of L_c on the basis of Gauss distribution (n is an amount of MOD particles)

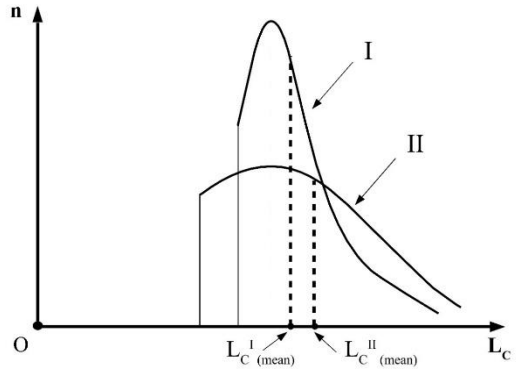

Fig. 16. An assumed distribution of L_c after the reaction (n is an amount of MOD particles)

The main thing in relation to distribution is that a value of L_c can increase after the reaction because an amount of small MOD decreases faster than the amount of larger MOD.

In our opinion, this is confirmed by [13] where coke going through a blast furnace increases the value of L_c. Further, the larger MOD with a larger L_c significantly influences coke strength and CSR (Fig. 17). An amount of bonds is larger with larger MOD than with small MOD (Fig. 17). Body of coke is stronger with a large amount of bonds between MOD.

On the basis of the assumed distribution, we can explain the deviation of the group from the general trend of CSR (Fig. 14). For example, values of L_c for 56.3 and points of 61.0–62.3 are approximately equal. We assume that the distribution of I in Fig. 14 is the coke with CSR of 56.3 and the distribution of II in Fig. 14 is the coke with CSR of 61.0–62.3 with the 61.7 mean (Fig. 15). A mean value of L_c for I and II is constant, but a mean square deviation of I is less than II (Fig. 15). An amount of larger MOD in II is larger than I, the coke of II is stronger than the coke of I. In theory, at a constant CRI (or the constant surface area as in Fig. 14), L_c of II is larger than L_c of I after the reaction (Fig. 16).

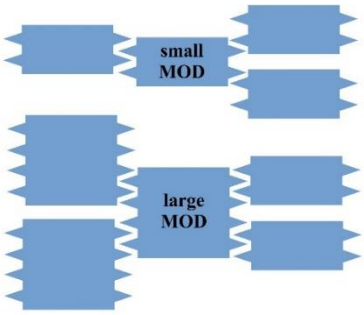

Fig. 17. A geometrical bond between larger and small MOD

3.3.2 Influence and physical interpretation of the coefficient r'_0

The coefficient r'_0 is included in formulas of m_1 and m_2 (equations I and III) and has correlation with CRI and CSR. On the basis of r'_0, we guess that the physical characteristics influencing both CRI and CSR may exist. The model permits to select similar curves of $CSR = f(CRI)$ with variations of r'_0 and A (Figs. 18 and 19) at constant remaining parameters.

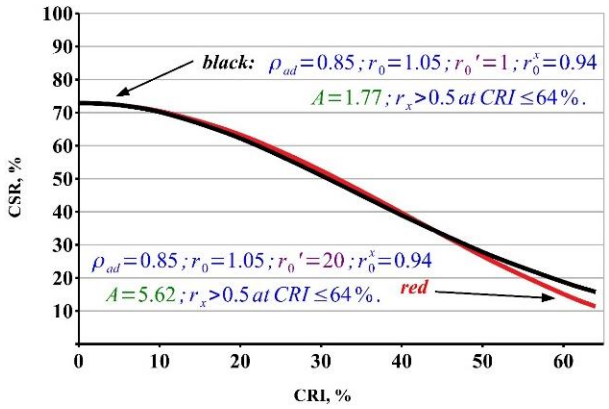

Fig. 18. An example of similar curves of $CSR = f(CRI)$ with variations of r'_0 and A

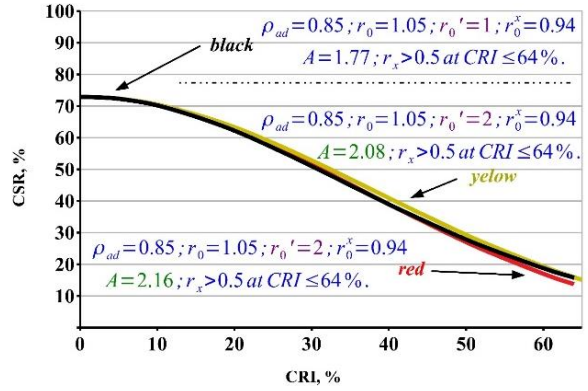

Fig. 19. An example of similar curves of $CSR = f(CRI)$ with variations of r'_0 and A

Fig. 20 and 21 are apparent density distributions for curves from Fig. 18, analogical to those in Figures 2 and and A.5 (Appendix A). The alteration of apparent density at $r'_0 = 20$ evenly takes place throughout the coke piece (Fig. 20).

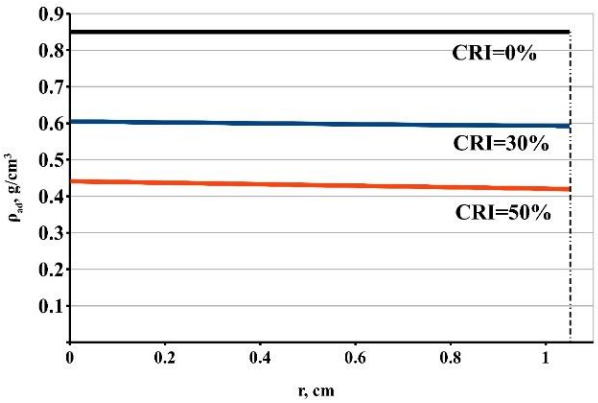

Fig. 20. The alteration of the apparent density depending on radius of a coke piece with the variation of CRI (corresponds to fig. 18 with a curve of $r'_0 = 20$). $r = 0$ is the center of a coke piece, $r = 1.05$ cm is the outside of a coke piece

At $r'_0 = 1$, the larger apparent density alteration is determined closer to the outside of a coke piece (Fig. 21). Analogous results can be obtained from the equation (A.39) differentiated by time (the formula (1) is (A.39)):

$$\rho(r) = kr + (\rho_{ad} + kr'_0) = k(r + r'_0) + \rho_{ad} \quad (1)$$

$$\frac{d\rho(r)}{d\tau} = (r + r'_0)\frac{dk}{d\tau} + k\frac{dr'_0}{d\tau} \quad (2)$$

At $dk = 0$ and $k = const$, from (2) to (3) (Fig. 22):

$$\frac{d\rho(r)}{d\tau} = k\frac{dr'_0}{d\tau} \quad (3)$$

At $dr'_0 = 0$ and $r'_0 = const$, the formula (2) transforms to (fig. 23):

$$\frac{d\rho(r)}{d\tau} = (r + r'_0)\frac{dk}{d\tau} \quad (4)$$

If the rate of the apparent density alteration depends more on $\frac{dr'_0}{d\tau}$, a variation of coke mass is constant both in the center and on the periphery of a coke piece after the reaction (fig. 24).

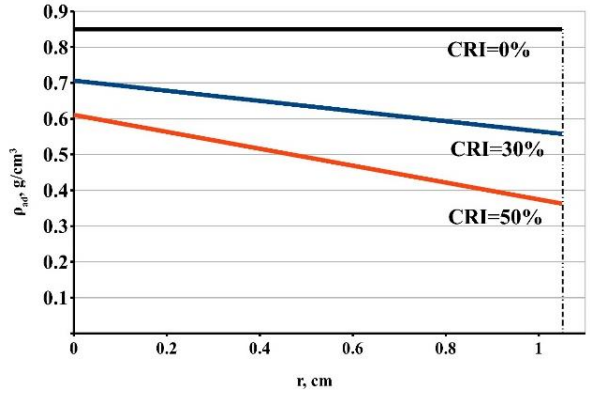

Fig. 21. The alteration of the apparent density depending on the radius of a coke piece with the variation of CRI (corresponds to fig. 18 with a curve of $r'_0 = 1$). $r = 0$ is the center of a coke piece, $\boldsymbol{r} = 1.05$ cm is the outside of a coke piece.

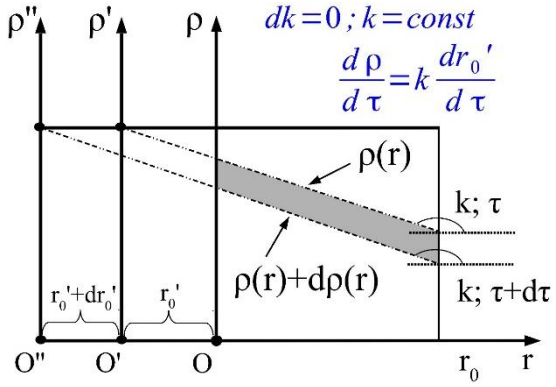

Fig. 22. An alteration of the apparent density depending on the radius of a coke piece (corresponds to formula 3)

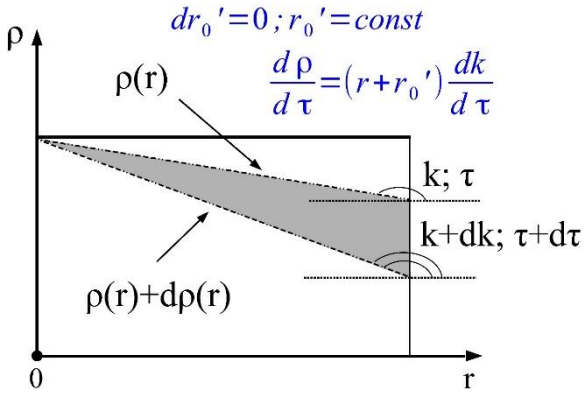

Fig. 23. An alteration of the apparent density depending on the radius of a coke piece (corresponds to formula 4)

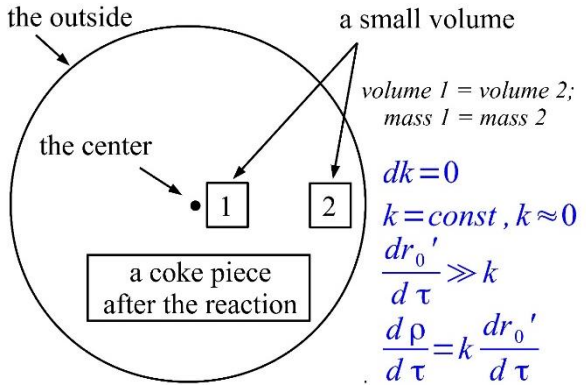

Fig. 24. A variation of mass in the center and the outside of a coke piece by formula (3)

If the rate of the apparent density alteration depends more on $(r + r'_0)\frac{dk}{d\tau}$, a variation of mass in a coke piece is non uniform. The mass loss of a coke piece closer to the outside is larger than in the center (Fig. 25). Consequently, the coefficient of r'_0 "is responsible" both for the uniformity and the rate of the apparent density alteration within a coke piece during the reaction. The uniformity can be determined by the amount of open pores (Fig. 26).

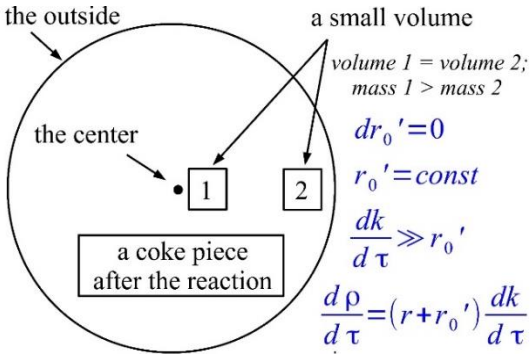

Fig. 25. A variation of mass in the center and the outside of a coke piece by formula (4)

We imply that an open pore is the pore oriented from the outside to the center of a coke piece with a minimum length (Fig. 27). In practice, we propose that an estimation of an amount of open or closed pores might be performed by means of the ratio of pore volume to pore surface area (V/S) within a coke piece. Hydraulic resistance of pores is less when the ratio is larger and CO_2 comes to the center of a coke piece (Figs. 22, 24 and 27).

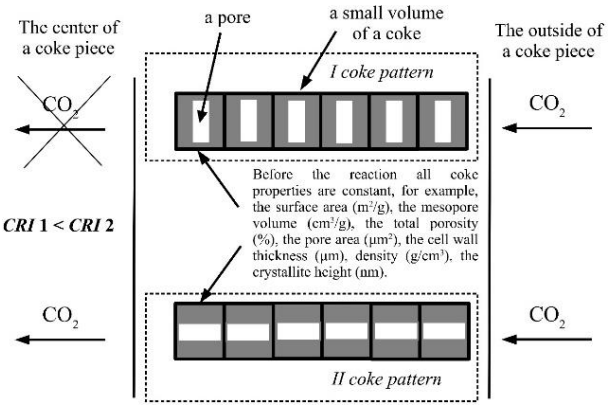

Fig. 26. The influence of a geometric pore orientation on CRI and CSR at constant physical properties of a coke piece

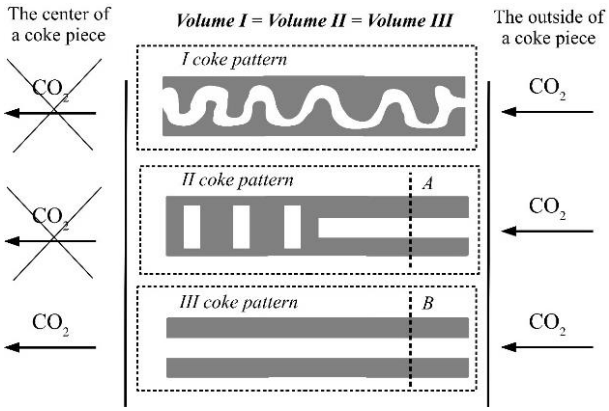

Fig. 27. A possible orientation of pores within a piece of coke. I coke pattern is a pore with high hydraulic resistance; II coke pattern is the closed pore; III coke pattern is an open pore

If the ratio is constant for two hypothetical samples, a variation of coke mass depends on the value of pore surface area. The physical measurement of open or closed pores' amount is given in [14].

Returning to the coefficient of r'_0, the dimension of r'_0 is in cm. On the one hand, in the model, r'_0 is a part of a hypothetical coke piece radius with the total radius of $r'_0 + r_0$ (Appendix A). The larger the value of r'_0, the more CO_2 reaches the r'_0 radius of a hypothetical coke piece with a radius of $r'_0 + r_0$. On the other hand, a variation of coke mass depends on the surface area in the course of the reaction because the reaction is heterogeneous. In the model, the physical meaning of k represents pores' surface area closer to the outside of a coke piece (Fig. 23), but the coefficient k relates to r'_0 in (I) and the seventh step of the algorithm (section 2.2). To summarize, the physical meaning of r'_0 is the total pores' surface area ***access*** during the reaction in a coke piece. The total surface area consists of the surface area closer to the coke outside (S_{BET}) and an ***available*** part from the surface area (S_{BET}) for the reaction within a coke piece (see Fig. 27), taking into account the coke piece mass [18, 19]. A variation of CRI can be expressed on the basis of r'_0 (Fig. 28).

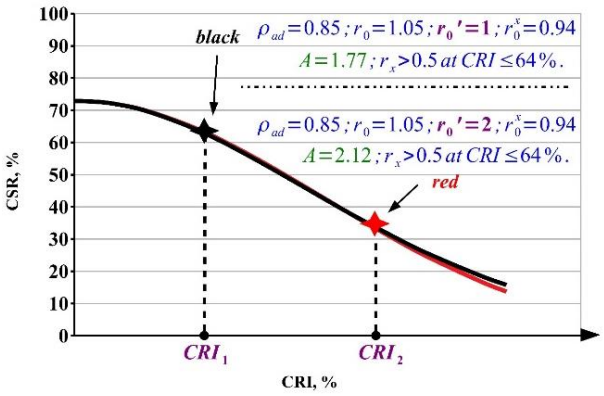

Fig. 28. A variation of CRI from r'_0. CRI_1 with $r'_0 = 1$; CRI_2 with $r'_0 = 2$; $CRI_2 > CRI_1$ because $r'_0 = 2 > r'_0 = 1$

Let us explain why we vary both parameters r'_0 and A (Fig. 28). In formula (I), m_1, and, therefore, CRI in formula (IV), depends on k and r'_0 (Fig. A.6 in Appendix A). The problem is that if we change r'_0, then k changes with constant CRI (formulas (I) and (V)). Mathematically, we can fix A and build a curve (formulas (II) - (IV)), but physically this will be wrong. Physically, the coefficient A arises when there is k. The more the straight line of apparent density tilts downward, the lower the apparent density (highly porous structure), the greater the coefficient A, that is, the coke breaks down more easily. Therefore, we select straight lines close to each other with different A and r'_0. Knowing that r'_0 affects CRI, we say that on the common curve CSR = f (CRI) for two pieces of coke, a point with $r'_0 = 2$ will have a point with a higher CRI than when $r'_0 = 1$. As we have established, r'_0 affects the mass change in the volume of a piece of coke (Fig. 22–25). Then the pattern in Figure 28 is logical. The deeper the reaction takes place, the greater the available surface area for the reaction, the greater the CRI, the more the coke body is weakened, the greater is A (Fig. 13). That is, Figure 28 reflects the physical order of the ongoing processes of mass loss and CRI, CSR while reacting with CO_2.

One of physical meanings of the coefficient r'_0, the uniformity of the apparent density alteration estimated from an amount of open pores can provide explanations to variations of CRI and CSR in different scale laboratory ovens. In small ovens, coke oven gas quickly evaporates from a small chamber with a small coal charge and the coke has a large amount of open pores (see our term "open pore"). In larger ovens, coke oven gas slowly evaporates because of a high hydraulic resistance with a large coal charge and escapes through large pores with a low hydraulic resistance. Evaporating slowly from the large chamber, coke oven gas can undergo the pyrolysis that clogs pores. Therefore, coke quality is better within larger ovens [15, 16]. The similar case is the variation of coke quality depending on the location of coke inside the industrial coking chamber [11, 20]. On the basis of an amount of open pores and the coefficient of r'_0, unsatisfactory correlation between coke quality and carbon coke forms' quantitative analysis can be explained [11, 17, 18]. For example, two patterns of II and III have identical carbon forms (Fig. 27, sections A and B), but pattern III is with open pores, while pattern II is with closed pores. At identical carbon forms for two coke patterns, r'_0 of III is larger r'_0 of II and CRI of III does as well, while CSR of II is larger than CSR of III (Figs. 26, 27 and 28).

In summary, in our opinion, coefficients of the model have physical meanings:

$$A = f(L_c) \quad \text{(a)}$$

$$r'_0 = f\left(S_{BET}, \frac{V}{S_{BET}}, m_{cp}\right) \quad \text{(b)}$$

$$k = f(S_{BET}) \quad \text{(c)}$$

$$CRI = f\left(S_{BET}, \frac{V}{S_{BET}}, m_{cp}\right) \quad \text{(d)}$$

$$CSR = f\big(CRI, f(L_c)\big) = f\left(S_{BET}, \frac{V}{S_{BET}}, m_{cp}, f(L_c)\right) \quad \text{(e)}$$

were L_c is a distribution of L_c; V – a volume of pores, cm^3/g; m_{cp} is the mass of a coke piece.

3.3.3 The collation of the fourth hypothesis with experimental data

Fig. 29 shows results of modelling the well-known relationship demonstrated in Fig. A.4. in Appendix A.

The model does not reproduce curves of $CSR = f(CRI)$ reaching to the red rectangle (Fig 29). For this reason, several points from fig. A.4. in Appendix A do not lie on the curves calculated by the model, for example, the point with $CRI = 70\%$ and $CSR = 10\%$. On the basis of the fourth hypothesis, we estimated the mass of one coke piece in a 200 g sample with $CRI = 70\%$ and $CSR = 10\%$.

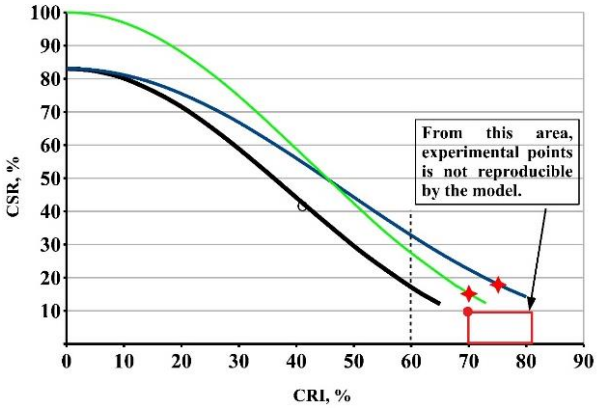

Fig. 29. Modelling of the relationship demonstrated in Fig A.4. (Appendix A)

The mass of coke pieces, remaining from a 200 g sample after the reaction, is:

$$\frac{200 * (100 - CRI)}{100} = 200 * 0{,}3 = 60\ g$$

The mass of coke pieces after the drum test is:

$$\frac{60 * CRS}{100} = 60 * 0{,}1 = 6\ g$$

If the mass of one coke piece is approximately 4 g (see Example 1 in Appendix A), a 200 g sample contains about 50 pieces. For one piece of coke from 50, mass after the drum test is:

$$\frac{6}{50} = 0{,}12g = 120\mu g$$

In the ISO-test, coke pieces should have diameter of at least 1 cm (radius of 0.5 cm). Within a 200 g sample with $CRI = 70\%$ and $CSR = 10\%$, in the model by the fourth hypothesis, one coke piece from a 200 g sample after the ISO-test is a sphere with a diameter of about 1 cm and the mass of $120\mu g$. Physically, we suppose that the dimension of 1 cm is too small for a coke piece with the mass of $120\mu g$ after the drum test. Minimally the model gives a curve reaching to the point with $CRI = 70\%$ and $CSR = 16\%$ (Fig. 29). At the same time, by the fourth hypothesis, the mass of a coke piece with $CRI = 70\%$ and $CSR = 16\%$ is $180\mu g$ with a piece diameter of at least 1 cm. By analogy, the mass of $180\mu g$ is too small for a physical body with a diameter of 1 cm after machining in the drum.

Experimental points within the red rectangle (Fig. 29 and Fig. A.4. in Appendix A) can be explained by the fact that a 200 g sample consists of coke pieces with poor and high quality. For instance, the study of [8] demonstrates that coke pieces within a 200 g sample have a significant variation of CRI. A variation of CRI induces a variation of CSR by the model. Thus, $CRI = 70\%$ and $CSR = 10\%$ values are the result of several coke pieces from a 200 g sample (Fig. A.4. in appendix A) in the ISO-test, the remaining coke pieces from a 200 g sample go through the screen.

4. Conclusions

We created and studied the model which reproduces the curves of $CSR = f(CRI)$ in the experimental data range of CRI and CSR. The following results are made on the basis of the model:

1) A larger part of the $CSR = f(CRI)$ curve is linear;
2) The universal regression by type $CSR = a + b * CRI$ does not exist;
3) Between pieces of coke, variation of CRI and CSR values can be explained by the open pore quantity, the pores' surface area, the statistical distribution of molecular oriented domains on the basis of L_c and the coke piece mass;
4) A geometrical pore orientation is the critical factor. Pores with a minimum length oriented from the outside to the center of a coke piece significantly influence CRI and CSR indexes.
5) Every coke piece is unique by CRI and CSR indexes and that creates an ancillary variation of CRI and CSR values during the ISO-test.

Acknowledgments

Danil Alekseev would like to thank associate professor Olga Solovieva for all-round help and support.

Appendix A. The mathematical analysis

The increment of a coke piece mass after the reaction with CO_2 is:

$$dm = \rho(r)dV \quad \text{(A.1)}$$

where $\rho(r)$ is coke apparent density, g/cm^3. In hypothesis 1 (section 2.1.), a coke piece for the ISO-test is a sphere and the coke volume increment depending on radius is:

$$dV = d\left(\frac{4}{3}\pi r^3\right) = 4\pi r^2 dr, \quad \text{(A.2)}$$

The equation (A.1) and (A.2) can be transformed to:

$$dm = 4\rho(r)\pi r^2 dr \quad \text{(A.3)}$$

r is a ball (spherical) radius.

From hypothesis 2 (section 2.1.), the general equation of relation between apparent density $\rho(r)$ and r is:

$$\rho(r) = kr + b \quad \text{(A.4)}$$

where k and b are empirical coefficients ($b = \rho_{ad}$ in Fig. 2 and Fig. 3).

The equation of (A.3) with (A.4) is:

$$dm = 4\pi(kr + b)r^2 dr \quad \text{(A.5)}$$

According to the hypothesis 3 (section 2.1.), the integral of 0 over r_0 for the (A.5) equation is:

$$\int_0^m dm = \int_0^{r_0} 4\pi(kr + b)r^2 dr \quad \text{(A.6)}$$

From (A.6) to (A.7), we can get the mass of a coke piece after the reaction:

$$m_1 = \frac{4\pi}{3} r_0^3 \left(k\frac{3r_0}{4} + b\right) = 4\pi\left(k\frac{{r_0}^4}{4} + b\frac{{r_0}^3}{3}\right) \quad \text{(A.7)}$$

The CRI and CSR indexes within the ISO standard are:

$$CRI = 100\frac{m_0 - m_1}{m_0} \quad \text{(A.8)}$$

$$CSR = 100\frac{m_2}{m_1} \quad \text{(A.9)}$$

Where m_0 is a 200 g sample, g;
m_1 is the sample mass after the reaction, g;
m_2 is mass of coke pieces with a size larger than 10 mm after machining in the drum.

From formulas (A.8) and (A.9) it is clear, CRI and CSR indexes within the 200 g sample are percentages, which can be used for changing the mass of a single coke piece (hypothesis 4, section 2.1.). From this in (A.8) and (A.9), m_0 is mass of a coke piece before the reaction, m_1 is mass of a coke piece after the reaction, m_2 is mass of a coke piece with a size larger than 10 mm after rotating in the drum, and CRI and CSR values are determined by means of the ISO-test for a 200 g coke sample. Below, Example 1 (with determined CRI and CSR values) demonstrates how to calculate by means of formulas (A.7) and (A.9).

Example 1. With $CRI = 30.0\%$ *and* $CSR = 60.0\%$, *we calculate the coke piece radius* r_x *after rotating in the drum. We assume that* $\rho_{ad} = 0.85$ *g/cm*^{3}, *and the initial radius of a coke piece is* $r_0 = 1.05$ *cm (see Figs. 1–3). The mass of one piece of coke will be:*

$$m_0 = V * \rho_{ad} = \frac{4}{3}\pi {r_0}^3 * \rho_{ad} = 4.122\ g$$

m_1 and k from formulas (A.8) and (A.7):

$$m_1 = m_0 - \frac{CRI * m_0}{100} \quad (A.10)$$

$$k = \frac{m_1}{\pi * {r_0}^4} - \frac{4}{3}\frac{b}{r_0} \quad (A.11),$$

Values of m_1 *and* k *at* $CRI = 30.0\%$ *and* $CSR = 60.0\%$ *(in conformity with Figs. 2 and 3 at* $b = \rho_{ad}$*):*

$$m_1 = m_0 - \frac{CRI * m_0}{100} = 4.122 - \frac{30 * 4.122}{100} = 2.885\ g$$

$$k = \frac{m_1}{\pi * {r_0}^4} - \frac{4}{3}\frac{b}{r_0} = \frac{2.885}{3.1416 * 1.05} - \frac{4}{3} * \frac{0.85}{1.05} = -0.324$$

Within the drum, the coke piece radius decreases from r_0 *to* r_x *(Fig. 3), and the mass of a coke piece is:*

$$m_2 = 4\pi\left(k\frac{{r_x}^4}{4} + b\frac{{r_x}^3}{3}\right) \quad (A.12)$$

On the other hand, the mass of a coke piece after rotating in the drum will be equal to (see formula (A.9)):

$$m_2 = \frac{m_1 * CSR}{100} \quad (A.13)$$

For this example, at $CRI = 30.0\%$ *and* $CSR = 60.0\%$*:*

$$m_2 = \frac{m_1 * CSR}{100} = \frac{2.885 * 60}{100} = 1.731\ g$$

Formula (A.12) consistent with (A.13) is:

$$\pi k\frac{{r_x}^4}{4} + \frac{4}{3}\pi b{r_x}^3 - \frac{m_1 * CSR}{100} = 0$$

This is a nonlinear equation with respect to the variable r_x *(*π *– Pi,* $k = -0.324$, $b = \rho_{ad} = 0.85$*;* $m_2 = \frac{m_1 * CSR}{100} = 1.731\ g$*).* $r_x = 0.86$ *cm is the solution. With value of* $r_x = 0.86 > 0.5$ *cm (*$d > 10$ *mm), a coke piece will remain on the screen with a cell of 10 mm.*

From the equations (A.10) – (A.13) it follows:

$$CRI = f(k) = linear(k) \quad (A.14)$$

$$CSR = f(k, r_x) = f(linear(k), nonlinear(r_x)) \quad (A.15)$$

$$CSR = f(linear(k), nonlinear(r_x)) = f(linear(CRI), nonlinear(r_x)) \quad (A.16)$$

Figure A.1. illustrates the relation between k and r_x. An increment of k induces an increment of r_x. We suggest that k and r_x variate by dk and dr_x, respectively.

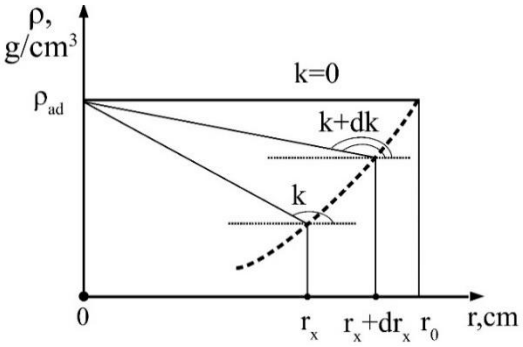

Fig. A.1. The illustration of k and r_x increments

The slope ratio value of k decreases when CRI increases ($k < 0$, equations of (A.4), (A.10)–(A.11)).

An apparent density distribution mitigated by the slope ratio of k ($k < 0$) induces that pores' wall thickness decreases and reduces the coke strength after the drum test and that is indicated by r_x and CSR (see Fig. 3 and A.1., formulas (A.14) and (A.15)). Geometrical relation between k and r_x is represented in Fig. A.2. If the angle of $d\varphi$ approaches to zero, then ΔABC and ΔMBN are isosceles, and $MN \parallel AC$ (Fig. A.2.).

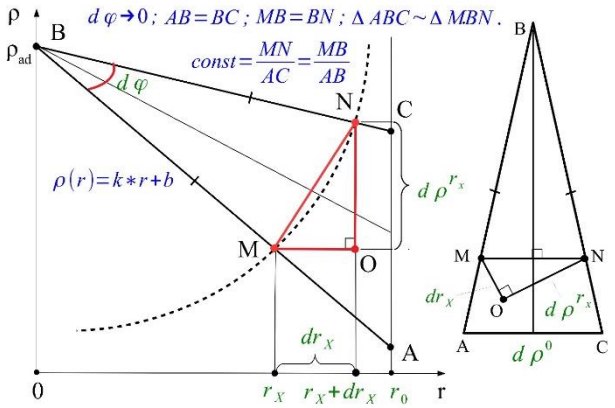

Fig. A.2. Geometrical relation between k and r_x

Triangles are similar:

$$\Delta ABC \sim \Delta MBN$$

From similar triangles to:

$$const = \frac{MN}{AC} = \frac{MB}{AB} \quad (A.17)$$

The triangle of ΔMON is rectangular by constructing. In the triangle ΔMON by the Pythagorean theorem:

$$MN^2 = (dr_x)^2 + (d\rho^{r_x})^2 \quad (A.18)$$

Formula of the apparent density at point of N (Fig. A.2.) is:

$$\rho^{r_x}(k, r_x) = k * r_x + b \quad (A.19)$$

Formula (A.19) in differential form is:

$$d\rho^{r_x}(k, r_x) = r_x dk + k dr_x \quad (A.20)$$

Then (A.18) transforms to:

$$MN^2 = (dr_x)^2 + (r_x dk + k dr_x)^2$$

$$MN = \sqrt{(dr_x)^2 + (r_x dk + k dr_x)^2} \quad \text{(A.21)}$$

Value of AC (Fig. A.2.):

$$\mathrm{AC} = d\rho^0 \quad \text{(A.22)}$$

Formula of $d\rho^0$ is:

$$\rho^0(k) = k * r_0 + b \quad \text{(A.23)}$$

$$d\rho^0 = r_0 * dk \quad \text{(A.24)}$$

With respect to (A.24) the formula (A.22) is as follows:

$$\mathrm{AC} = r_0 * dk \quad \text{(A.25)}$$

The values of MB and AB can be written by means of the formula of the curve length from mathematical analysis:

$$\mathrm{d}s = \sqrt{1 + \left(\frac{d\rho}{dr}\right)^2}\, dr = \sqrt{1 + \left(\frac{d(kr+b)}{dr}\right)^2}\, dr = \sqrt{1+k^2}dr \quad \text{(A.26)}$$

$$s = \int_0^{\kappa} \sqrt{1+(k)^2} dr = r * \sqrt{1+k^2} \quad \text{(A.27)}$$

The variable of r_0^x has a physical meaning in (A.33). If a coke going to the ISO-test with $CRI = 0$ is rotated in the drum, the coke can be crushed and have the CSR≤100% (at $CRI = 0$, $k = 0$; Fig. A.3.). That is $r_0^x \leq r_0$ at $k = 0$.

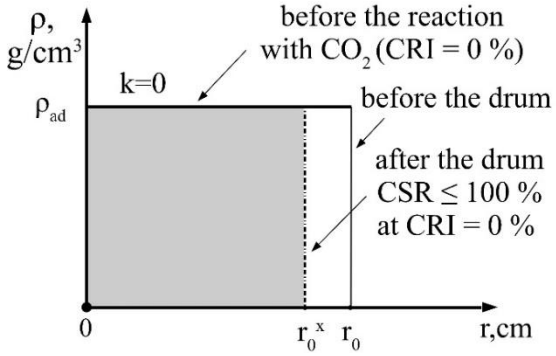

Fig. A.3. – Illustration of the physical meaning of r_0^x

The integral (A.33) is:

$$ln\frac{r_x}{r_0^x} = -ln\, t = ln\frac{1}{t} = \ln\frac{1}{1+k^2}$$

$$r_x = r_0^x * \frac{1}{1+k^2} \quad \text{(A.34)}$$

While reasoning we suggested that the increment of dk induces the increment of dr_x. As a matter of fact, the increments of dk and dr_x can be with a coefficient of proportionality. That's why we enter the coefficient of A:

$$r_x = r_0^x \frac{1}{1+(A*k)^2} \quad \text{(A.35)}$$

Formula (A.35), confirmed by Fig. 3 and (A.11) – (A.12), is not universal for the entire experimental range of CSR and r_x. Example 2 confirms this fact at $CRI = 70\%$ and $CSR = 20\%$ (Fig. A.4.).

Example 2. The point of this example is radius of a coke piece with $CRI = 70\%$ and $CSR = 20\%$. The mass of one piece of coke is:

$$m_0 = V * \rho_{ad} = \frac{4}{3}\pi {r_0}^3 * \rho_{ad} = 4.122\ g.$$

After the reaction:

$$MB = r_x * \sqrt{1+k^2} \quad \text{(A.28)}$$

By analogy:

$$AB = r_0 * \sqrt{1+k^2} \quad \text{(A.29)}$$

With (A.21), (A.24), (A.28) and (A.29), (A.17) transforms to:

$$\frac{\sqrt{(dr_x)^2+(r_x dk+k dr_x)^2}}{r_0 * dk} = \frac{r_x * \sqrt{1+k^2}}{r_0 * \sqrt{1+k^2}}\ , \text{(A.30)}$$

After mathematical transformations, from (A.30) to:

$$\frac{dr_x}{r_x} = -\frac{2kdk}{1+(k)^2} \quad \text{(A.31)}$$

After the change of a variable in (A.31):

$$\mathrm{t} = 1 + (k)^2;\ dt = 2kdk;\ if\ \ k = 0\ then\ t = 1 \quad \text{(A.32)}$$

With respect to (A.32), (A.31) is:

$$\frac{dr_x}{r_x} = -\frac{dt}{t}$$

$$\int_{r_0^x}^{r_x} \frac{dr_x}{r_x} = -\int_1^t \frac{dt}{t} \quad \text{(A.33)}$$

$$m_1 = m_0 - \frac{CRI * m_0}{100} = 4.122 - \frac{70 * 4.122}{100} = 1.237\ g$$

$$k = \frac{m_1}{\pi * {r_0}^4} - \frac{4}{3}\frac{b}{r_0} = \frac{1.237}{3.1416 * 1.05} - \frac{4}{3} * \frac{0.85}{1.05} = -0.756$$

The coke piece abrades in the drum and its radius decreases from r_0 to r_x. The mass of the coke piece after the drum test is:

$$m_2 = \frac{m_1 * CSR}{100} = \frac{1.237 * 20}{100} = 0.2473\ g$$

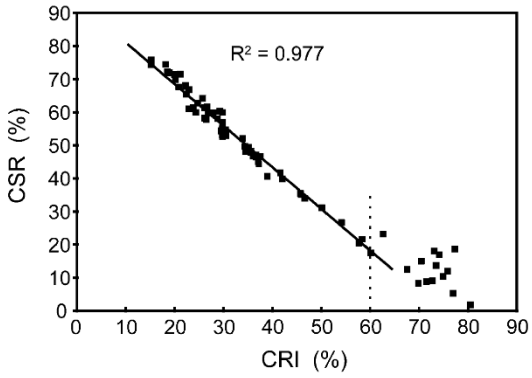

Fig. A.4. Interrelation between CRI and CSR indexes [7]

Formula (A.12) combined with (A.13) leads to:

$$\pi k\frac{{r_x}^4}{4} + \frac{4}{3}\pi b {r_x}^3 - 0.2473 = 0$$

This is a nonlinear equation with the variable r_x (π – Pi, $k = -0.756$, $b = \rho_{ad} = 0.85$). $r_x = 0.46$ cm is the solution. With a value of $r_x = 0.46 < 0.5$ cm ($d < 10$ mm), all sampled coke pieces are under screen with a cell of 10 mm which is not true ($CSR = 20\%$).

This inadequacy can be explained by the fact that the apparent density in the coke center ($r = 0$) is variable (Fig. A.5.).

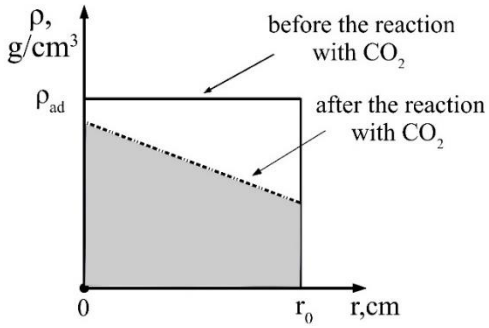

Fig. A.5. General case of the apparent density distribution depending on radius in a piece of coke

Thus, the linear distribution in Fig. A.5. is the general case in comparison with the particular case given in Fig. 2. For realizing the general case in (A.35), axis of ρ must go to ρ' as shown in Fig. A.6. In the coordinate system of $\boldsymbol{\rho' 0' r}$, formula (A.35) is:

$$R_x = R_0^x \frac{1}{1+(A*k)^2} \quad \text{(A.36)}$$

$$R_x = r'_0 + r_x;\ R_0^x = r'_0 + r_0^x \quad \text{(A.37)}$$

where r'_0 is an empirical coefficient.

Taking into account (A.37), a formula (A.36) is:

$$r_x = r_0^x \frac{1}{1+(A*k)^2} + r'_0 \left(\frac{1}{1+(A*k)^2} - 1\right) \quad \text{(A.38)}$$

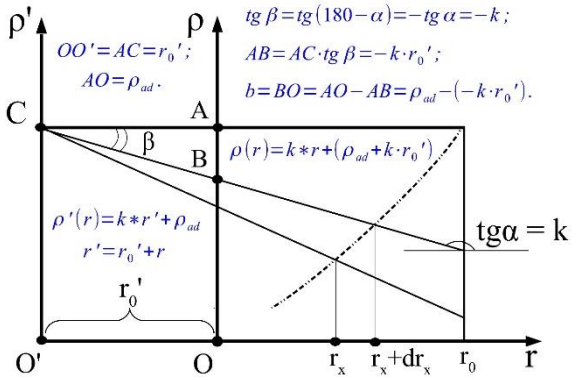

Fig. A.6. The linear distribution of the apparent density in a coke piece after the reaction (Fig. A.6. is a composite of Fig. 2, A.1 and A.5.)

Formula (A.4) for the general case (Fig. A.6) is:

$$\rho(r) = kr + b = k(r + r'_0) + \rho_{ad} = kr + \\ +(\rho_{ad} + kr'_0) \quad \text{(A.39)}$$

With respect to (A.38) and (A.39) formula (A.16) equals to:

$$CSR = CSR(linear(CRI), nonlinear(r_x)) = \\ CSR(linear(CRI), nonlinear(CRI; A; r'_0; r_0^x)) \quad \text{(A.40)}$$

With the coefficient of r'_0 in (A.38), Example 2 has a value of $r_x > 0.5$ at $CRI = 70\%$ and $CSR = 20\%$ which is true.

Appendix B. Argumentation of hypothesis 2

In our opinion, the hypothesis 2 is both debatable and poorly studied within the realm of similar hypotheses (section 2.1). Below we estimate other distributions of the apparent density depending on the coke radius and compare them with the general case of a linear distribution (Fig. A.6, formula (A.39)).

B.1. Coke reacts with CO_2 exclusively on the outer surface of a coke piece

In this section we make an assumption that coke reacts with CO_2 solely on the outer surface of a coke piece (Fig. B.1.) but not in the volume of a coke piece (hypothesis of 3, section 2.1.).

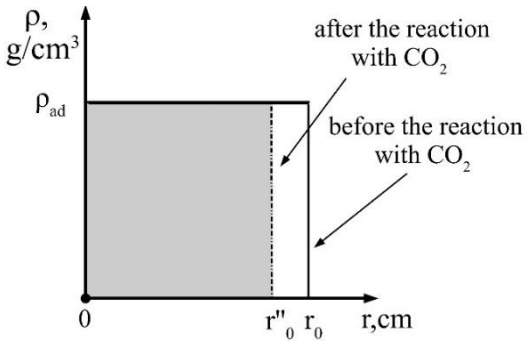

Fig. B.1. Distribution of the apparent density $\rho(r)$ depending on radius if coke reacts with CO_2 exclusively on the outer surface of a coke piece

In view of this assumption (Fig. B.1.) we calculate the radius of the coke after the reaction at $CRI = 30\%$ (by analogy with Example 1):

$$m_0 = V * \rho_{ad} = \frac{4}{3}\pi {r_0}^3 * \rho_{ad}$$

$$m_1 = m_0 - \frac{m_0 * CRI}{100} \text{ (see formula of (A.10));}$$

$$m_1 = \frac{4}{3}\pi {r''_0}^3 * \rho_{ad}$$

$$\frac{4}{3}\pi {r''_0}^3 \rho_{ad} = \frac{4}{3}\pi {r_0}^3 \rho_{ad} - \frac{4}{3}\pi {r_0}^3 \rho_{ad} * \frac{CRI}{100}$$

$${r''_0}^3 = {r_0}^3 - {r_0}^3 \frac{CRI}{100}$$

$$r''_0 = r_0 \sqrt[3]{1 - \frac{CRI}{100}}$$

At $CRI = 30\%$

$$r''_0 = r_0 \sqrt[3]{1 - \frac{CRI}{100}} = 1.05 \sqrt[3]{1 - \frac{30}{100}} = 0.93\ cm$$

$$d = 2r''_0 = 2 * 0.88 = 1.86\ cm = 18.6\ mm$$

According to the ISO-test coke pieces must be sized at about 20 mm. Together with other researchers we observe coke shape retention after the reaction in practice (hypothesis of 3, section 2.1). However, practically the apparent density distribution can be as given in Fig. B.2., analogical to Fig.B.1., as well as 1, 3-5 hypotheses, excluding the hypothesis 2 (section 2.1).

The apparent density distribution of (a) (Fig. B.2.) can be observed in practice if the reaction rate of coke with CO_2 is limited by the diffusion of CO_2 and CO between kernel gas flow in the ISO-reactor and the coke piece outer surface.

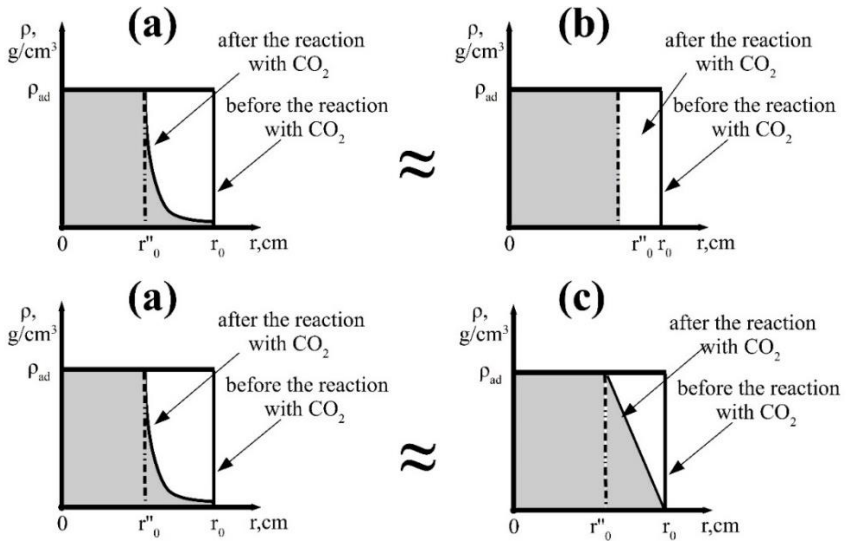

Fig. B.2. Possible variations in the apparent density distribution after the reaction if coke reacts with CO2 solely on the outer surface of a coke piece

For the ISO-test (three stages, section 2.1), on the basis of any apparent density distributions, the material balance of the coke piece can be calculated. The material balance (m_0, m_1 and m_2 at different CRI) of the coke piece can be compared with the experimental values of CRI and CSR and with a trend of $CSR = f(CRI)$. Approximately, the distribution of (a) is the distribution of (c) in Fig. B.2. For the distribution of (c), the material balance is estimated by the model at $r'_0 < 0$.

The model gives m_2 with an overestimation at $r'_0 < 0$ (Fig. B.3, the red area). We calculated the material balance by the model at $r'_0 = -0.5$. From the material balance, we calculated CRI and CSR indexes (formulas (A.5) and (A.6); hypothesis of (4) in section 2.1.). Calculated values of CRI and CSR beyond experimental data of CRI and CSR are not physical. The calculated trend of $CSR = f(CRI)$ has a U-shape form which is false compared with an experimental linear trend. In our opinion, the preservation of a coke piece shape and radius after the reaction as well as calculated values of CRI and CSR (beyond experimental data of CRI and CSR) demonstrate that coke reacts within the entire volume of a coke piece, including its inner surface (Fig.B.2. is false).

B.2. Coke reacts within the entire volume of a piece, including its inner surface, but the apparent density distribution is nonlinear

The apparent density distribution can be represented as:

$$\rho(r) = \omega(-r + r_n)^{\frac{1}{c}} \quad \text{(B.1)}$$

Where $c > 1$, ω and r_n are empirical coefficients. Nonlinear effect increases by large coefficient of c. The coefficient of c is arbitrary.

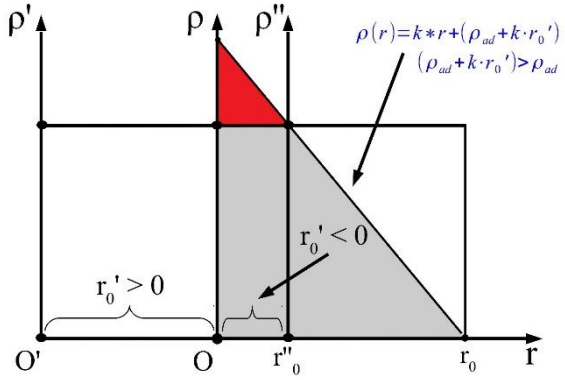

Fig. B.3. Overestimation for m_2 according to the model at $r'_0 < 0$ (red area)

If:

$$\rho(0) = \rho_{ad}$$

Then:

$$\omega = \frac{\rho_{ad}}{r_n^{\frac{1}{c}}}$$

The coefficient of r_n is calculated by m_1:

$$m_1 = m_0 - \frac{CRI * m_0}{100}$$

$dm = \rho(r)dV$ (formula (A.1) in Appendix A)

$$dm = \omega(-r + r_n)^{\frac{1}{c}}dV = \frac{\rho_{ad}}{r_n^{\frac{1}{c}}} * (-r + r_n)^{\frac{1}{c}}dV$$

$$dV = d\left(\frac{4}{3}\pi r^3\right) = 4\pi r^2 dr$$

$$dm = \omega(-r + r_n)^{\frac{1}{c}}dV = 4\pi\frac{\rho_{ad}}{r_n^{\frac{1}{c}}} * (-r + r_n)^{\frac{1}{c}}r^2 dr$$

$$\int_0^{m_1} dm = \int_0^{r_0} 4\pi\frac{\rho_{ad}}{r_n^{\frac{1}{c}}} * (-r + r_n)^{\frac{1}{c}}r^2 dr$$

$$m_0 - \frac{CRI * m_0}{100} = \int_0^{r_0} 4\pi \frac{\rho_{ad}}{r_n^{\frac{1}{c}}} * (-r + r_n)^{\frac{1}{c}} r^2 dr$$

$$m_0 - \frac{CRI * m_0}{100} = \int_0^{r_0} 4\pi \frac{\rho_{ad}}{r_n^{\frac{1}{c}}} * (-r + r_n)^{\frac{1}{c}} r^2 dr$$

We set the values of m_0, CRI, c, and select the coefficient r_n in such a way that the above equation is fulfilled.

For example, at c = 4, $m_0 = 4.122\ g$ and $CRI = 30\%$ (see Example 1), linear and nonlinear distributions are:

$$linear: \rho(r) = -0{,}324r + 0{,}85$$

$$nonlinear: \rho(r) = 0{,}83(-r + 1{,}1)^{\frac{1}{4}}$$

The results of the calculations on the basis of (B.1) are shown in Fig. B.4. [18].

A nonlinear distribution is hard to use for the analyses of material balance during the ISO-test. Besides, a nonlinear distribution does not provide any new information about the ISO-test.

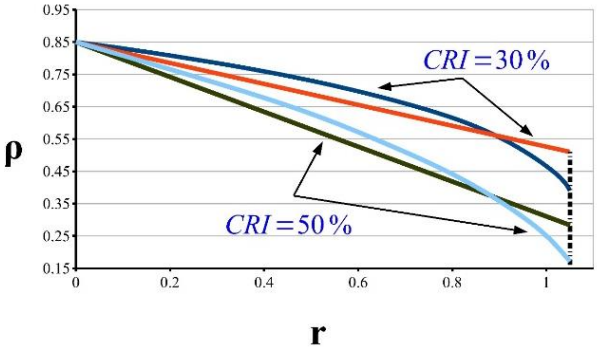

Fig. B.4. Comparison of linear and nonlinear distributions of the apparent density depending on a coke piece radius (at $m_0 = 4.122\ g$)

References

1. Lipatnikov, AV., Shmelyova, AE. et. al. Mathematical modeling and optimization of raw coal consumption in PJSC «MMK». Vestnik Magnitogorskogo Gosudarstvennogo Tekhnicheskogo Universiteta im. G.I. Nosova 16(4), 30–38 (2018), DOI: https://doi.org/10.18503/1995-2732-2018-16-3-30-38.
2. North, L., Blackmore, K. et. al. Methods of coke quality prediction: A review. Fuel 219, 426–445 (2018), DOI: https://doi.org/10.1016/j.fuel.2018.01.090.
3. North, L., Blackmore, K. et. al. Models of coke quality prediction and the relationships to input variables: A review. Fuel 219, 446–466 (2018), DOI: https://doi.org/10.1016/j.fuel.2018.01.062.
4. Smirnov, AN., Petukhov VN., Alekseev DI. Classification of models for predicting coke quality (M25 and M10). Coke Chem 58(5), 170–174 (2015), DOI: https://doi.org/10.3103/S1068364X15050087.
5. Wang, Q., Guo, R. et. al. A new testing and evaluating method of cokes with greatly varied CRI and CSR. Fuel 182, 879–885 (2016), DOI: http://dx.doi.org/10.1016/j.fuel.2016.05.101.
6. Shelkov AK: Reference book of a cokemaker. Volume 2. Production of coke. Metallurgy, Moscow, 1965.
7. Dıez, MA., Alvarez, R., Barriocanal, C. Coal for metallurgical coke production: predictions of coke quality and future requirements for cokemaking. Int J Coal Geol. 50(1–4), 389–412 (2002), DOI: https://doi.org/10.1016/S0166-5162(02)00123-4.
8. Koval, L., Sakurovs, R. Variability of metallurgical coke reactivity under the NSC test conditions. Fuel 241, 519–521 (2019), DOI: https://doi.org/10.1016/j.fuel.2018.12.053.
9. Pusz, S., Buszko, R. Reflectance parameters of cokes in relation to their reactivity index (CRI) and the strength after reaction (CSR), from coals of the Upper Silesian Coal Basin, Poland, Int J Coal Geol. 90–91, 43–49 (2012), DOI: https://doi.org/10.1016/j.coal.2011.10.008.
10. Zolotukhin, YuA., Andreichikova, NS., Koshkarovb, DA. Relationship between CSR and CRI and comparison of these parameters for box and commercial cokes. Coke Chem. 50(1), 15–18 (2007), DOI: https://doi.org/10.3103/S1068364X07010048.
11. Nyathi, MS., Kruse, R. et. al. Nature and origin of coke quality variation in heat-recovery coke making technology. Fuel 176, 11–19 (2016), DOI: http://dx.doi.org/10.1016/j.fuel.2016.02.050.
12. Smędowski, Ł., Krzesińska, M. et. al. Development of ordered structures in the high-temperature (HT) cokes from binary and ternary coal blends studied by means of X-ray diffraction and Raman spectroscopy. Energy Fuels 25(7), 3142–3149 (2011), DOI: https://doi.org/10.1021/ef200609t.
13. Gupta, S., Ye, Z. et. al. Coke graphitization and degradation across the tuyere regions in a blast furnace. Fuel 113, 77–85 (2013), DOI: http://dx.doi.org/10.1016/j.fuel.2013.05.074.
14. Sakurovs, R., Koval, L. et. al. Nanostructure of cokes, Int J Coal Geol. 188, 112–120 (2018), DOI: https://doi.org/10.1016/j.coal.2018.02.006.
15. Tiwari, HP., Banerjee, PK. et. al. Efficient way to use of non-coking coals in non-recovery coke making process. Metall Res Technol. 111(4), 211–220 (2014), DOI: https://doi.org/10.1051/metal/2014026.
16. Mahoney, M., Andriopoulos, N. et. al. Pilot scale simulation of cokemaking in integrated steelworks. Ironmak Steelmak 32(6), 468–478(2005).
17. Nyathi, MS., Kruse, R. et. al. Investigation of coke quality variation between heat-recovery and byproduct cokemaking technology. Energy Fuels 27, 7876–7884 (2017), DOI: https://doi.org/10.1021/acs.energyfuels.6b02817.
18. Huang, J., Guo, R. et.al. Coke solution-loss degradation model with non-equimolar diffusion and changing local pore structure. Fuel 263, 116694(2020), DOI: https://doi.org/10.1016/j.fuel.2019.116694.

19. Numazawa, Y., Saito, Y. Large-scale simulation of gasification reaction with mass transfer for metallurgical coke: Model development. Fuel 266, 117080 (2020), DOI: https://doi.org/10.1016/j.fuel.2020.117080.
20. Flores BD., Borrego AG. et. al. How coke optical texture became a relevant tool for understanding coal blending and coke quality. Fuel Process Technol, 164, 13–23 (2017), DOI: https://doi.org/10.1016/j.fuproc.2017.04.015.